RSC Advances

PAPER

View Article Online
View Journal | View Issue

Cite this: *RSC Adv.*, 2017, **7**, 12886

pH-sensitive polymeric micelles for the Co-delivery of proapoptotic peptide and anticancer drug for synergistic cancer therapy†

Anbu Mozhi,[abc] Israr Ahmad,[bc] Chukwunweike Ikechukwu Okeke,[abc] Chan Li*[abc] and Xing-Jie Liang*[abc]

Received 20th November 2016
Accepted 8th February 2017

DOI: 10.1039/c6ra27054a

rsc.li/rsc-advances

Mitochondria plays a vital role in a wide range of biological processes in human health and diseases. They are considered to be important organelles responsible for cellular apoptosis or programmed cell death. Therefore, the targeting of chemotherapy towards mitochondria would be highly desirable. Herein, we developed a pH-sensitive polymer that is designed for the subcellular co-delivery of anticancer drugs and therapeutic peptides to tumor cells. The amphiphilic copolymer poly(β-amino esters)-poly(ethylene glycol) was synthesized and conjugated with the dual-targeting proapoptotic peptide CGKRK$_D$(KLAKLAK)$_2$. The conjugate can self-assemble into a core–shell micellar structure at the physiological pH of 7.4. The anticancer drug docetaxel (DTX) was encapsulated inside the core of the micelles. The CGKRK peptide is specifically targeted to angiogenic blood vessels in tumors and tumor cells, whereby the micelles are efficiently internalized into tumor cells *via* an energy-dependent, lipid draft/caveolae-mediated endocytosis pathway. Once inside the acidic endosomal compartment, the stimuli-responsive micellar carriers disassemble and release both pharmacological agents. CGKRK efficiently transports $_D$(KLAKLAK)$_2$ towards mitochondria to trigger mitochondria-dependent apoptosis. DTX affects microtubulin for arresting the cancer cell cycle. Thus, the combination of DTX and the therapeutic peptide displayed a synergistic antitumor effect in an MCF-7 cell line.

1 Introduction

The formation of a new vascular network is an important key factor for the proliferation as well as metastatic spread of cancer. The creation of new blood vessels from pre-existing vessels by means of a process is defined as angiogenesis.[1–5] Hence, targeting angiogenic blood vessels would be considered to be a distinct feature of the treatment of cancer. The cell surface and extracellular matrix of tumor blood vessels express various specific protein markers that normal cells do not express or express at much lower levels in comparison with tumor cells.[6] Hereby, receptors on the surface of angiogenic cancer cells are prone to anchor target-specific circulating moieties such as antibodies, small biomolecules, DNA, aptamers, and peptides.[7–9] Hence, the respective ligands have high targeting ability to deliver drugs or macromolecules to tumor vasculature or tumor cells and thereby reduce systemic toxicity by limiting the exposure of healthy cells.[10,11] Like other chemotherapy treatments, anti-angiogenic therapy has not provided long-lasting therapeutic efficacy for the shrinkage of tumor cells. To overcome this issue, researchers designed and developed a ligand that can play a dual-targeting role in tumor blood vessels and tumor cells. Therefore, the dual-targeting peptide not only cuts off the blood vessels that supply nutrients and oxygen to the tumor but also directly kills the tumor cells after anti-angiogenic therapy.[12]

The CGKRK (Cys-Gly-Lys-Arg-Lys) peptide was recognized by *in vivo* screening.[13] This peptide sequence was found to have high affinity and specific target-binding ability for the interior surface of angiogenic tumor blood vessels and tumor cells.[14] The mitochondrial protein p32, which is considered to be the receptor of CGKRK peptide, is expressed at higher levels on the surface of various cancer cells than on that of healthy cells.[15] Therefore, the mechanism of the cellular internalization of CGKRK peptide into tumor cells was recognized as an energy-dependent and receptor-mediated endocytosis pathway.[16,17]

The proapoptotic D-amino acid peptide KLAKLAKKLAKLAK ($_D$(KLAKLAK)$_2$) is a cationic α-helical amphipathic mitochondrial membrane-disrupting peptide that can initiate apoptotic cell death. Basically, this peptide is used as an antibacterial peptide to damage the bacterial cell membrane, but on the other hand it experiences difficulties in crossing the eukaryotic

[a]*Laboratory of Controllable Nanopharmaceuticals, Chinese Academy of Sciences (CAS), Zhongguancun, Beijing 100190, China. E-mail: lic@nanoctr.cn; liangxj@nanoctr.cn; Fax: +86-010-62656765; Tel: +86-010-82545569*

[b]*Key Laboratory for Biomedical Effects of Nanomaterials and Nanosafety, National Center for Nanoscience and Technology, No. 11, First North Road, Zhongguancun, Beijing 100190, China*

[c]*University of Chinese Academy of Sciences, Beijing 100049, China*

† Electronic supplementary information (ESI) available. See DOI: 10.1039/c6ra27054a

plasma membrane. Hence, it is less toxic to eukaryotic cells.[18,19] To enhance the role of the $_D$(KLAKLAK)$_2$ peptide in killing cancer cells, researchers have combined the CGKRK peptide sequence as a tumor-specific binding ligand with the $_D$-(KLAKLAK)$_2$ peptide.[20–23] Here, the peptide segment CGKRK acts on angiogenic tumor blood vessels and the $_D$(KLAKLAK)$_2$ sequence disrupts mitochondrial membranes and serves as a drug to kill cancer cells *via* an apoptosis pathway.[24] When it is in soluble form, the peptide sequence exhibits a significant systemic toxic effect, even when it is specifically designed for targeting tumors.[25] To find a solution, the peptide has been chemically conjugated to a nanosystem to reduce its toxicity.[26,27]

In contrast to other nanoparticles, in recent years polymeric nanoparticles have gained much more attention in cancer research as drug delivery systems. The intracellular compartments of tumor cells are characterized by different pH values. Healthy cell environments, the extracellular matrix and blood have a pH value of around 7.4, whereas inflammatory and cancer cells usually have slightly elevated acidity, with a pH of 6.5–7.2. This might be because of the poor supply of oxygen to their intracellular space. Even greater differences in pH can be experienced in the subcellular regions of tumors; endosomes and lysosomes have lower pH values in the range of 5.0–6.0.[28–30] Therefore, these acidic conditions make pH-sensitive polymers ideal candidates for cancer treatment. In 2000, Langer *et al.* were the first to synthesize poly(β-amino esters) as a nanocarrier for a gene delivery system.[31] Later, some researchers have used poly(β-amino esters) for drug delivery and also as a combined drug/gene delivery system.[32,33] Apart from this, few researchers have modified therapeutic peptides with pH-sensitive polymers for cancer chemotherapy.

Here, we have developed a pH-sensitive poly(β-amino ester)-poly(ethylene glycol) copolymer (PBAE-PEG) conjugated to the proapoptotic therapeutic peptide CGKRK$_D$(KLAKLAK)$_2$. This can aggregate into a nanomicellar system having PBAE as an inner core and poly(ethylene glycol) (PEG) as an outer shell to prolong the life of the nanomicelles during circulation in serum. To enhance their therapeutic efficacy in cancer, the hydrophobic drug docetaxel (DTX) was loaded inside the core (Scheme 1A). Such self-assembled polymeric micelles are directly targeted towards the tumor vasculature and are internalized efficiently *via* a receptor-mediated endocytosis pathway. Under acidic conditions the micelles disassemble and release their therapeutic payloads. CGKRK localizes the $_D$(KLAKLAK)$_2$ peptide towards the mitochondria to damage the mitochondrial membrane for the induction of apoptosis, and DTX kills the cancer cells, which results in synergistically enhanced apoptosis (Scheme 1B). Finally, the combined co-delivery of the therapeutic peptide and DTX *via* polymeric micelles can increase the pharmacological payload of anticancer agents inside the tumor regions and thereby enhance their therapeutic efficacy during cancer chemotherapy.

2 Materials and methods

2.1 Chemicals and reagents

1,4-butanediol diacrylate (BD) and 5-amino-1-pentanol (AP) were received from Alfa Aesar. mPEG-NH$_2$ (Mw = 2000 Da) was obtained from Sigma Aldrich. The D-amino acid CGKRK$_D$(-KLAKLAK)$_2$ peptide sequence was synthesized by GL Biochem (Shanghai, China), and its purity was verified by HPLC (≥95%).

The human breast cancer cell line MCF-7 was purchased from the American Type Culture Collection (ATCC; Manassas, VA). Dulbecco's modified Eagle's medium (DMEM) and fetal bovine serum (FBS) were purchased from HyClone (USA). 3-(4,5-dimethylthiazol-2-yl)-2,5-diphenyltetrazolium bromide (MTT) was bought from Promega Corporation (USA). Trypsin–EDTA solutions were purchased from Gibco (Life Technologies, Canada), and penicillin and streptomycin were bought from Invitrogen (The Netherlands). Culture dishes and plates were obtained from Corning (New York, USA). LysoTracker Green (LysoTracker), the JC-1 assay kit and DAPI were supplied by Thermo Fisher Scientific, Inc. Deionized water (DI water) was obtained from a Milli-Q water purification system (Millipore, France), and phosphate-buffered saline (PBS, 10 mM, pH 7.4) was used for drug release experiments and cell studies. Other chemicals and reagents were used as received from the suppliers.

2.2 Synthesis and conjugation of therapeutic peptide-polymer

The PBAE-PEG (PP) copolymer was polymerized as follows: in brief, BD (943 mg, 5 mmol), AP (408 mg, 3.74 mmol), and mPEG-NH$_2$ (832 mg, 0.416 mmol) were mixed and dissolved in 2 mL dry DMSO. The polymerization reaction was performed in a dark inert atmosphere at 50 °C for a week with mechanical stirring. The reaction was stopped and the system brought down to room temperature. Unreacted monomers were removed by washing three times with an excess amount of cold ether. Furthermore, the PBAE-PEG (PP) copolymer was allowed to dry under vacuum for 24 h. The chemical structure of acrylate-terminated PBAE-PEG (PP) was characterized by ^{1}H NMR spectrometry (400 MHz) in a d^6-DMSO solvent.

To conjugate the therapeutic peptide sequence, PP (100 mg, 0.0225 mmol) and CGKRK$_D$(KLAKLAK)$_2$ (TP) (150 mg, 0.075 mmol) were uniformly dispersed in 2 mL dry DMSO. The mixture was left undisturbed with magnetic stirring in an inert atmosphere at 50 °C for 5 d. After completion of the reaction, the mixture was purified by dialysis against water (M_W cut-off: 2 kDa), and dried samples were obtained by lyophilization. To confirm the conjugation of the therapeutic peptide to the acrylate-terminated PBAE-PEG (PP), ^{1}H NMR spectrometry (400 MHz) was performed in a d^6-DMSO solvent. The molecular weights (M_n) of PBAE-PEG (PP) and CGKRK$_D$(KLAKLAK)$_2$-PBAE-PEG (TPPP) were confirmed by gel permeation chromatography (GPC) (Shimadzu LC-20A). The instrument was equilibrated to 40 °C and the measurements were conducted in a pre-filtered DMF solvent at a flow rate of 1.0 mL min^{-1}. Polystyrene was used as a standard for calibration.

2.3 Fabrication of docetaxel-loaded polymeric micelles

Blank micelles and docetaxel (DTX)-loaded micelles were prepared *via* dialysis. CGKRK$_D$(KLAKLAK)$_2$-PBAE-PEG (TPPP) (6 mg) and DTX (0.4 mg) were mixed well in 1 mL DMSO, and then

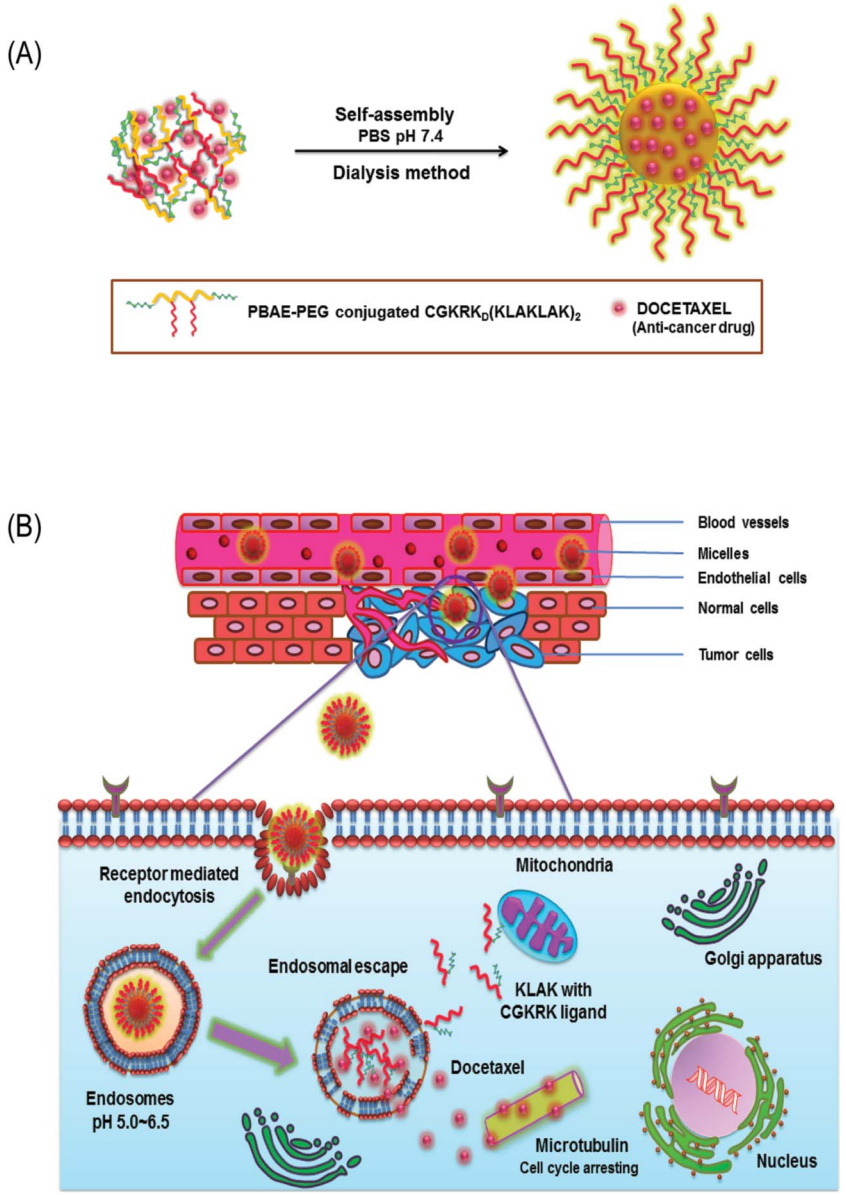

Scheme 1 Schematic of the drug-loaded polymeric micelles and their cellular uptake mechanism. (A) Self-assembly of docetaxel (DTX) with CGKRK$_D$(KLAKLAK)$_2$-conjugated PBAE-PEG copolymer at the physiological pH of 7.4. (B) Delivery of DTX and the therapeutic peptide by targeted micelles from the blood circulation into the tumor tissue and internalization of the targeted micelles by tumor cells *via* a receptor-mediated endocytosis pathway.

the organic phase was added dropwise to 2 mL PBS (pH 7.4) with gentle stirring for 2 h to allow the copolymers to self-assemble into micelles. Finally, the organic solvents were removed by dialysis against 1 L phosphate buffer (PBS) at a pH of 7.4. DTX-loaded PBAE-PEG (PP) micelles and blank micelles were also prepared in an identical procedure to that mentioned above. For fluorescence imaging studies, the fluorescent probe Cy5 was loaded into polymeric micelles without DTX.

2.4 Characterization of micelles

The hydrodynamic diameter and surface charge of micelles were determined with a dynamic light scattering (DLS) analyzer (Zetasizer Nano ZS). The morphology of the micellar structure was determined using a transmission electron microscope (Tecnai G2 20 S-TWIN). The TEM samples were prepared as follows: a 10 μL sample was dropped onto a TEM grid and excess solution was removed using filter paper after 5 min. Then, the sample was stained with 10 μL phosphotungstic acid (2%) solution for 40 s, followed by the removal of excess solution, and left undisturbed to dry.

2.5 Circular dichroism (CD) spectrum

The CD spectra of TP, PP micelles and TPPP micelles were recorded at room temperature using a circular dichroism

spectrometer (JASCO-1500, Japan). The samples were scanned at a speed of 1000 nm min^{-1} with a resolution of 0.5 nm.

2.6 pH sensitivity and critical micelle concentration (CMC)

The assembly and disassembly properties during micelle formation based on the pH and CMC of the polymeric sample were determined using pyrene as a fluorescent hydrophobic probe.[34] A solution of pyrene in acetone (1 mL) was dispersed into PBS solution, and then acetone was removed using a rotary evaporator at 60 °C for 1 h. The concentration of the pyrene solution was 1×10^{-7} M. The excitation (λ_{ex}) and emission (λ_{em}) wavelengths were 334 and 337 nm, respectively.

To determine the pH sensitivity of the polymer (2 mg mL^{-1}), a 0.1 M aqueous solution of HCl was gradually added to the solution of the polymer. After every addition, the sample reading was noted. The peak intensity at I_{337}/I_{334} was plotted against different pH values. The CMC of the micelles was determined by adding the polymer solution to PBS containing pyrene (pH 7.4). Different polymer concentrations were used during this study. The ratio of the intensity of the third to that of the first vibronic peak (I_{337}/I_{334}) *versus* the polymer concentration was used to draw a graph. An increase in the polymer concentration in the solution led to an increase in the intensity ratio, and finally at a certain point a plateau was observed. The CMC was calculated on the basis of the intersection of two lines obtained by linear regression.

2.7 Degradation study

The hydrolytic degradation of the TPPP copolymer was studied in buffer solutions with two different pH values (7.4 and 5.5), respectively. In detail, 10 mg polymer was added to 5 mL buffer. For 1 h the polymer solution was agitated and sonicated at 10 min intervals at room temperature and then shaken at 37 °C. After a predetermined time interval, polymer samples were collected and freeze-dried for GPC studies.

2.8 pH-dependent DTX release

The discharge profile of DTX from TPPP micelles was studied by dialysis in different buffer solutions (PBS, pH = 7.4 and acetate buffer, pH = 5.0). A dialysis bag was dropped into 50 mL buffer solutions with different pH values containing Tween-80 (0.5% w/v) as a solubilizer for hydrophobic DTX. The samples were then incubated in a shaker at a speed of 100 rpm. Samples were withdrawn at different intervals and replaced with the same amount of fresh medium. The discharged DTX was measured *via* HPLC. The drug encapsulation efficiency (EE) was also calculated by the same method.

2.9 *In vitro* cytotoxicity studies

MCF-7 cells were cultured in 96-well plates (7000 cells per well). After 24 h, they were incubated with free DTX, free TPPP micelles, DTX-loaded PP micelles, and DTX-loaded TPPP micelles at different concentrations, and cells without any drug treatment were used as a control group. After 24 h, the old medium in each well was removed, MTT solution was added, and the mixture incubated for a further 4 h. Then, 100 μL DMSO was added to each well to allow the formazan crystals to dissolve, and the absorbance was recorded at 570 nm (Tecan Infinite M200, Männedorf, Switzerland). All experiments were performed in triplicate.

2.10 Cellular uptake and intracellular distribution

For qualitative analysis of cellular uptake and endosomal escape, MCF-7 cells were seeded in 8-well chambered glass dishes (1.5×10^4 cells per well) and supplied with DMEM medium containing 10% FBS and 1% antibiotics (penicillin-streptomycin, 10 000 U/mL). After 24 h, the cells were incubated with TP + Cy5, Cy5-loaded PP micelles and Cy5-loaded TPPP micelles at different time intervals. The drugs were removed and the cells were rinsed with PBS three times. Soon after being washed, the cells were incubated with LysoTracker for 15-20 min in serum-free medium (1 : 1000 times dilution) and washed with PBS three times. After replacement with 300 μL PBS, they were observed by confocal laser scanning microscopy. Cy5 and LysoTracker Green DND-26 were excited at 650 nm and 488 nm, respectively.

2.11 Quantitative flow cytometry analysis

MCF-7 cells were cultured in 6-well plates (3×10^5 cells per well) and then incubated with Cy5, Cy5-loaded PP micelles and Cy5-loaded TPPP micelles for 3 h. Then, the old medium was poured off and the cells were rinsed with PBS three times. Then, the cells were trypsinized for collection in a centrifuge tube and replaced with 600 μL PBS to obtain a uniform suspension. The suspended cells were examined by a flow cytometer (Life Technologies).

2.12 Mitochondrial depolarization by JC-1 assay

Cancer cells were cultured in 8-well glass dishes (1.5×10^4 cells per well). After 24 h, the cells were incubated with $CGKRK_D$ $(KLAKLAK)_2$ (TP), PBAE-PEG (PP) micelles and $CGKRK_D$ $(KLAKLAK)_2$-PBAE-PEG (TPPP) micelles in DMEM medium (300 μL) supplemented with 10% FBS and 1% antibiotics. After 4 h, the cells were rinsed with PBS three times and incubated with 200 μL JC-1 dye (1 μL dye from stock + 5 μL DMSO + 1 mL serum-free medium) for 20 min. Then, the cells were rinsed thoroughly with PBS three times and viewed by confocal microscopy.

2.13 Endocytosis inhibition experiments

Cells were cultured in 8-well glass dishes (1.5×10^4 cells per well) for 24 h. Before treatment with micelles, cells were kept at 37 °C and 4 °C for 1 h and then Cy5-loaded micelles were incubated for 2 h. The cells were then rinsed thoroughly with PBS and immobilized using 2% paraformaldehyde solution for 20 min. After being rinsed with PBS three times, the nuclei of cells were stained with DAPI for 2 min (1 : 1000 times dilution with PBS). The medium was replaced with PBS and the cells were examined under a confocal microscope. The mechanism of cellular internalization of the micelles in MCF-7 cells was studied by pre-incubation for 1 h with different endocytosis inhibitors,

namely, 5 μg mL^{-1} chlorpromazine, 30 μg mL^{-1} genistein, and 2.5 mM methyl-β-cyclodextrin (M-β-CD). After the pretreatment, the micelles were incubated for 2 h and washed with PBS. The remaining procedures were the same as those mentioned above.

2.14 Observation of mitochondria by Bio-TEM

MCF-7 cells were treated with PP and TPPP micelles for 36 h. The cells were rinsed with PBS, trypsinized and collected in a 1.5 mL Eppendorf tube. After centrifugation for 3 min at 1000 rpm, the supernatant was poured off and the cells were immobilized with 2.5% glutaraldehyde (1 mL) at 4 °C overnight. After being rinsed thoroughly with PBS three times, the cells were further fixed with 1% osmium tetroxide for 2 h and were again rinsed with PBS three times. The cells were dehydrated in a graded ethanol series (50%, 60%, 70%, 80%, 90%, and 100%) and 100% acetone at room temperature, then immobilized in resin, and finally stored at 40 °C, 50 °C and 60 °C for 24 h. The immobilized samples were then slit into fine pieces with a thickness of 50-70 nm and stained with the negative stain uranyl acetate before observation.

2.15 Statistical analysis

All necessary experimental work was carried out in triplicate and the final results expressed as the mean ± standard deviation (SD). Statistical significance was examined using Student's *t*-test for two groups. *P*-values of <0.05 were considered to be significant.

3 Results and discussion

3.1 Characterization of therapeutic peptide-polymer

The PP copolymer was synthesized by Michael addition. In a single step, pH-sensitive and hydrophobic monomers were polymerized with hydrophilic mPEG-NH_2 to obtain amphiphilic properties, and could readily self-assemble to form micelles (Scheme 2). The molar feed ratio of BD to AP and mPEG-NH_2 was 1.2 : 0.9 : 0.1. Excess BD was necessary in the reaction to ensure that PP was terminated with acrylate for the subsequent conjugation with TP. To confirm the structure of acrylate-terminated PP, a ^{1}H NMR study was carried out. As shown in Fig. S1A† typical peak appeared at 5.91–6.39 ppm, which represented the terminal double bonds. The degree of polymerization (DP) of the PP copolymer was 8 units, which was predicted by ^{1}H NMR. The peak area of 'e' at ~4.0 ppm and the peak area of the acrylate group at ~6.2 ppm were used for calculating the DP of the copolymer. Similarly, the proton signals of mPEG at ~3.5 ppm and BD at ~4.0 ppm were utilized to calculate the degree of substitution by mPEG in the copolymer. The calculated integration ratio indicated that 10% were grafted, which was similar to the feed ratio during the reaction.

TPPP was synthesized by the conjugation of the activated thiol group in the peptide to acrylate-terminated PP at its terminal positions. As shown in the NMR spectrum in Fig. S1B,† the proton signal peak of acrylate at 5.91–6.39 ppm disappeared, and new peaks denoted by asterisks appeared. These new peaks were assigned to the conjugated $CGKRK_D(KLAKLAK)_2$ peptide by comparison with the NMR spectrum of the free peptide (Fig. S1C†). Thus, the result indicated that the $CGKRK_D(KLAKLAK)_2$ peptide was successfully linked to both ends of the copolymer chain. The results of gel permeation chromatography (GPC) shown in Fig. S2† revealed the number-average molecular weight (M_n) and PDI of PP and TPPP, which are displayed in Table S1.†

3.2 Physicochemical characterization of micelles

Transmission electron microscopy (TEM) observations provided clear evidence of the formation of PP micelles, which were spherical in nature, as shown in Fig. 1A. Fig. 1B reveals that the conjugation of the therapeutic peptide (TP) to PP caused an increase in the size of the micellar structures. After loading with 5.13% DTX, the size of the resulting micellar structures increased further, as shown in Fig. 1C.

As shown in Fig. 1D–F, and S3† and Table 1, DLS results revealed that the average hydrodynamic diameters of drug-free PP micelles, drug-loaded PP micelles, drug-free TPPP micelles and DTX-loaded TPPP micelles were 79 ± 1 nm, 83 ± 2 nm, 80 ± 1 nm and 117 ± 4 nm, respectively. A significant change in the charge of the micelles was also measured. Before conjugation with TP, the PP micelles exhibited charge that was close to neutral. After conjugation with cationic TP, the electrical charge moved towards the positive direction, which indicated the presence of TP in TPPP.

To prevent degradation by proteases, the $_D(KLAKLAK)_2$ peptide was synthesized from D-amino acids. The biological activity of the $_D(KLAKLAK)_2$ peptide is mainly dependent on its α-helical structure. To confirm this, the CD spectra of PP, TP, and TPPP micelles were investigated using standard CONTINLL algorithms.[35] The negative band of TP at 207 nm was shifted to 213 nm, which confirmed the conjugation of α-helical TP to the PP copolymer, as shown in Fig. 2.

3.3 Examination of pH sensitivity of copolymeric micelles

The pH-sensitive property of the polymeric material was obtained owing to the reversible protonation of tertiary amine groups on the backbone of the polymer chain, which have a pK_b of about 6.5.[36] The pH-dependent assembly and disassembly of polymeric micelles were studied by fluorescence spectroscopy using pyrene as a probe.[37] The hydrophobicity of the micelles was calculated on the basis of the I_{337}/I_{334} ratio at different pH values, as shown in Fig. 3A. At a low pH of 5.0–5.7, there was no obvious change in the I_{337}/I_{334} ratio, which indicated that the TPPP copolymer became hydrophilic and did not form micellar structures owing to the protonation of tertiary amine groups. When the pH was >5.7, the I_{337}/I_{334} ratio increased, which implied that the TPPP copolymer started to form micelles owing to the deprotonation of tertiary amine groups. When the pH was above 6.8, the I_{337}/I_{334} ratio reached a plateau, which indicated that the copolymer formed stable micelles in the extracellular environment. Fig. 3B illustrates that a solution of copolymeric micelles at a pH of 7.4 displayed obvious Tyndall light scattering, whereas at a pH of 5.0 there was no Tyndall effect, which is consistent with the disassembly of TPPP micelles at an acidic pH.

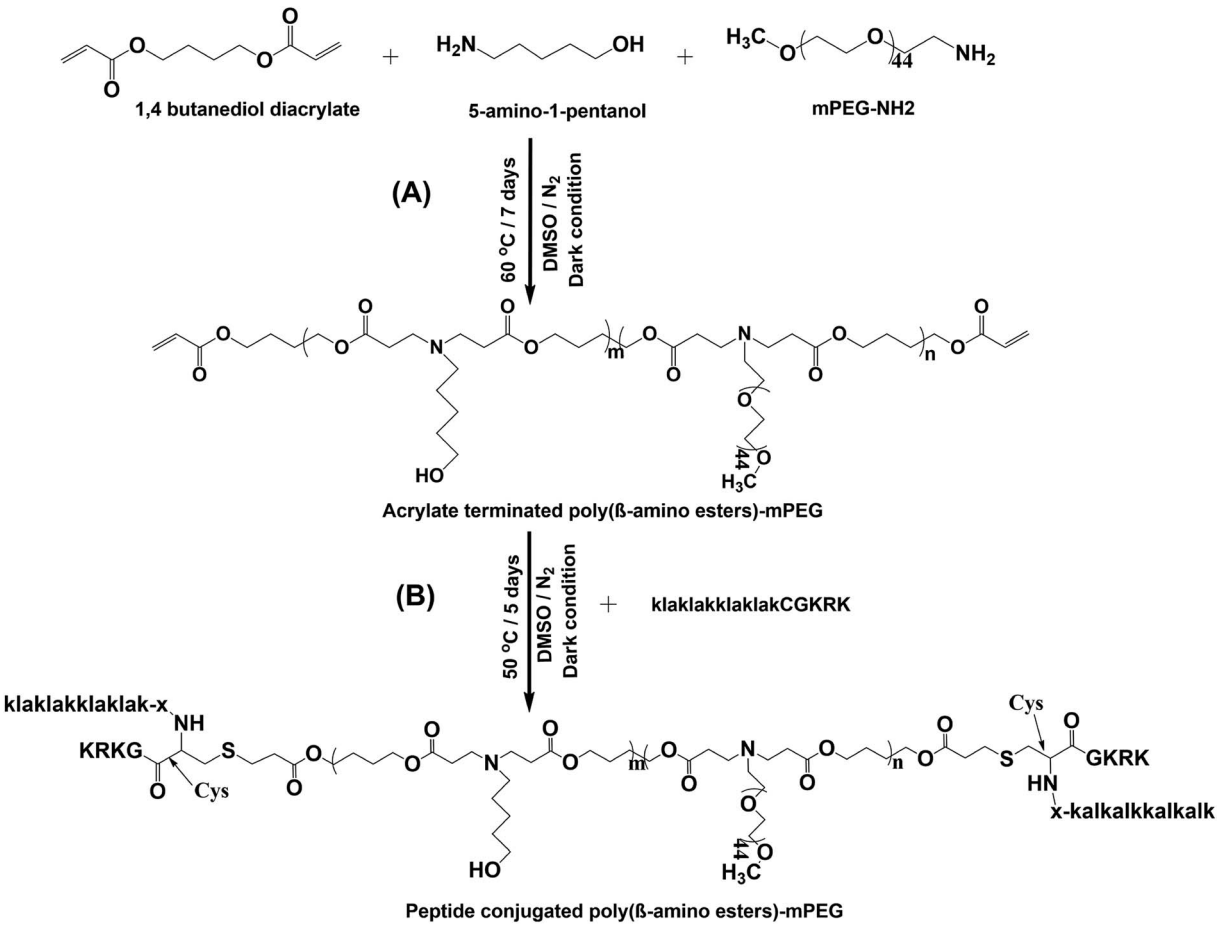

Scheme 2 Synthesis routes of (A) PBAE-PEG copolymer (PP) and (B) therapeutic peptide $CGKRK_D(KLAKLAK)_2$-conjugated PBAE-PEG copolymer (TPPP).

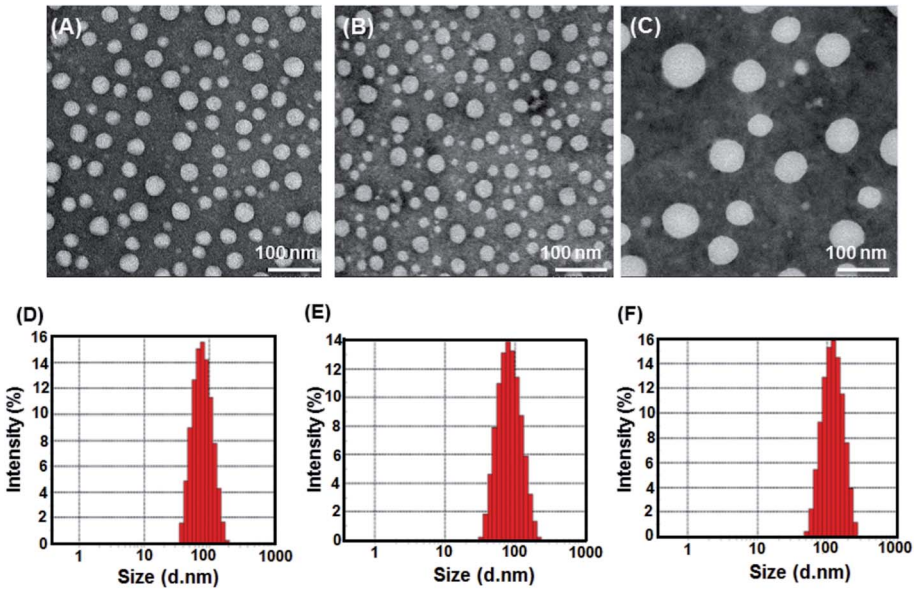

Fig. 1 TEM images and DLS plots of (A, D) drug-free PP micelles, (B, E) drug-free TPPP micelles and (C, F) DTX-loaded TPPP micelles.

Table 1 Physicochemical characterization of PP, DTX-loaded PP, TPPP and DTX-loaded TPPP micelles

Micelles	Particle size[a] (nm)	PDI[a]	Zeta potential[a] (mV)	Encapsulation efficiency[b] (%)	Loading content (%)
PP	79 ± 1	0.21	1.12	-	-
PP/DTX	83 ± 2	0.18	1.26	87	5.8
TPPP	80 ± 1	0.32	4.20	-	-
TPPP/DTX	117 ± 4	0.23	4.56	77.4	5.13

[a] Obtained from DLS measurements at a pH of 7.4 ($n = 3$). [b] Determined by HPLC ($n = 3$).

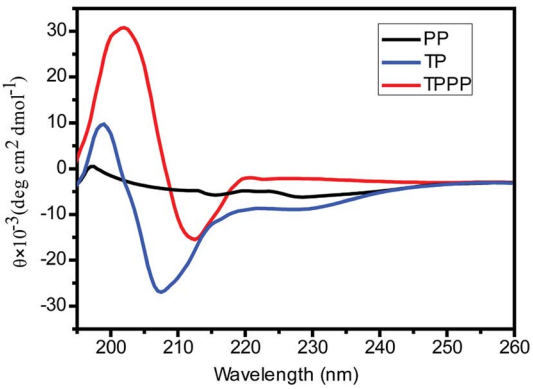

Fig. 2 CD spectra of PP, TP and TPPP micelles. PP = PBAE-PEG, TP = $CGKRK_D(KLAKLAK)_2$, TPPP = $CGKRK_D(KLAKLAK)_2$-PBAE-PEG.

3.4 Study of micelle formation and degradation

The CMC is an essential parameter for determining the stability of nanomicellar structures. On the basis of a technique reported earlier,[38] the CMC was determined in PBS buffer at a pH of 7.4. From Fig. 4 and Table S1,† the CMC of TPPP micelles was about 0.04 mg mL^{-1} and that of PP micelles was 0.01 mg mL^{-1}.

The degradability profile of the TPPP copolymer was investigated by monitoring the decrease in the molecular weight of the copolymer according to the incubation time in PBS at pH values of 7.4 and 5.5, respectively (see †). The degradation pattern of copolymer implies that the molecular weight of the polymer decreased continuously (Fig. S4C†). Degradation was faster at a pH of 5.5 than at a pH of 7.4, which might be due to the hydrolysis of pH-sensitive amino ester bonds in the backbone of the polymer chain. The hydrophobic PBAE polymer in the micelles remained insoluble at a pH of 7.4 and thereby prevented the rapid degradation of the copolymeric micellar system in physical environmental conditions.

3.5 pH-triggered release of DTX from micelles

The release behavior of DTX is plotted in Fig. 5. PBS at a pH of 7.4 was used as a release medium to simulate the environment of blood, and a pH of 5.5 was used to simulate the acidic environment inside the late endosomes of cancer cells. There was an initial burst release within 3 h, followed by subsequent sustained release. Only 10% of DTX was discharged at a pH of 7.4, which suggested that the DTX-loaded micelles were stable under physiological conditions. However, 80% of DTX was discharged in acid conditions, which might be due to the protonation of the PBAE segment and subsequent demicellization of the polymeric micelles in an acidic environment.

3.6 *In vitro* cytotoxicity

The cytotoxic effect of TP was investigated in a breast cancer cell line. The cells were incubated with various concentrations of the therapeutic peptide (TP). Fig. 6A shows that TP had an IC_{50} of about 830 μg mL^{-1}. Fig. 6B shows that at a concentration of 100 μg mL^{-1} PP^{-1} and TP did not have a toxic effect on cancer cells. In comparison with TP ($IC_{50} \approx 830$ μg mL^{-1}), the IC_{50} of TPPP was reduced by a factor of 14 to ~60 μg mL^{-1}. This means that the delivery of the therapeutic peptide by pH-sensitive micelles markedly enhanced its cytotoxicity to cancer cells.

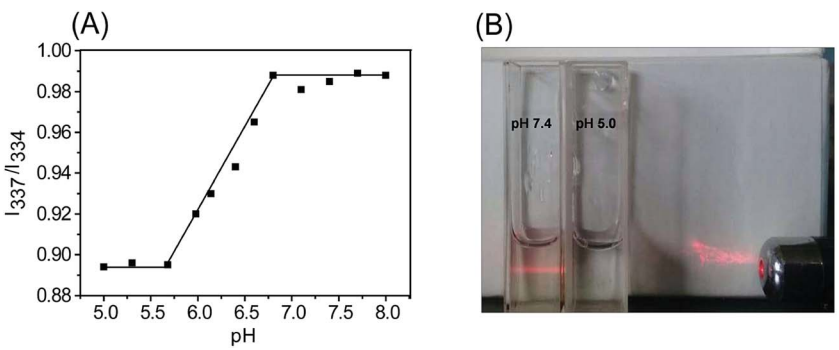

Fig. 3 (A) pH sensitivity of TPPP copolymer, I_{337}/I_{334} ratio of pyrene *versus* pH value. (B) Tyndall effect of TPPP copolymer in a buffer solution at different pH values. TPPP = $CGKRK_D(KLAKLAK)_2$-PBAE-PEG.

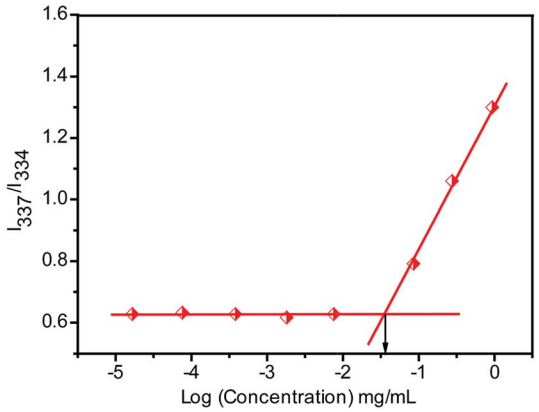

Fig. 4 CMC of TPPP nanomicelles obtained from a plot of the I_{337}/I_{334} ratio *vs.* the copolymer concentration in PBS buffer at a pH of 7.4.

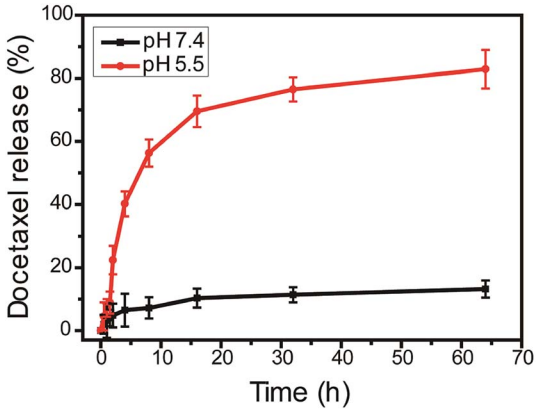

Fig. 5 pH-dependent discharge pattern of DTX from a TPPP ($CGKRK_D(KLAKLAK)_2$-PBAE-PEG) copolymeric nanosystem in phosphate buffer solution (pH 7.4) and sodium acetate buffer solution (pH 5.5).

The cytotoxicities of free DTX, TPPP, DTX-loaded PP, and DTX-loaded TPPP were determined and are represented in Fig. 6C. The final system had an IC_{50} value of ~0.5 μg mL^{-1}, which indicated that it exhibited an enhanced synergistic effect in killing cancer cells. The IC_{50} values of free DTX, DTX-loaded PP and empty TPPP micelles were ~5.1 μg mL^{-1}, ~3.6 μg mL^{-1} and ~2.6 μg mL^{-1}, respectively. This might be due to the target specificity of the therapeutic peptide conjugated to drug-loaded pH-sensitive micelles, which efficiently delivered a higher pharmacological payload inside the tumor cells. Thereby, the combined action of the released peptide and the drug exhibited a better anticancer effect in killing MCF-7 tumor cells.

3.7 Cellular uptake study

To investigate the cellular uptake and distribution of micelles in MCF-7 cells, PP and TPPP micelles were loaded with Cy5 dye and lysosomes were stained with LysoTracker Green DND-26. The mixture of TP + Cy5 could not pass through the cell membranes in 3 h. However, Cy5-loaded PP micelles entered the cells efficiently in 3 h, which can be observed in Fig. 7A, but within 1 h there was no obvious uptake of micelles by the cells, as shown in Fig. S5.† As shown in Fig. 7A, Cy5-loaded TPPP micelles displayed enhanced cellular uptake, which might be due to a difference in the endocytosis pathway. Furthermore, staining with LysoTracker indicated that the micelles were located in the lysosomal compartment and cytoplasm.

After incubation with polymeric micelles for 2 h, the mean fluorescence intensity of MCF-7 cells was quantitatively examined using flow cytometry. Fig. 7B and C demonstrate that the fluorescence signal corresponding to Cy5-loaded TPPP micelles was much stronger than those of free Cy5 and Cy5-loaded PP micelles. The difference in intracellular fluorescence intensity was due to the target specificity of the $_D(KLAKLAK)_2$ peptide.

3.8 Detection of mitochondria-regulated apoptosis

The loss of the mitochondrial transmembrane potential is the major feature of the promotion of apoptosis in cancer cells. As mentioned earlier, the cationic $_D(KLAKLAK)_2$ peptide has the ability to damage the membrane of mitochondria and initiate apoptotic cell death. In order to investigate mitochondria-regulated apoptosis, 5,5′,6,6′-tetrachloro-

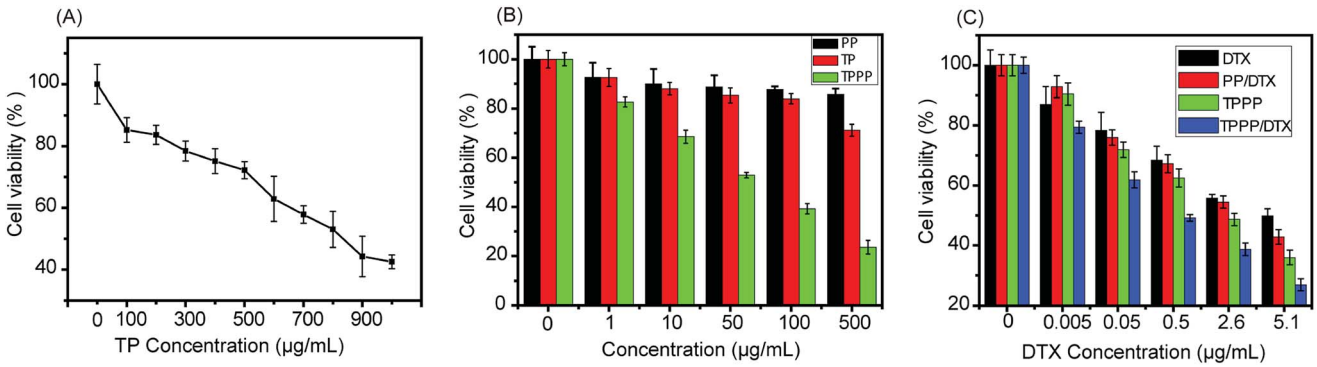

Fig. 6 (A) Viability of MCF-7 cells incubated with various concentrations of TP. (B) Cytotoxicity study on MCF-7 cells incubated with PP, TP and TPPP micelles; the concentrations of PP and TP were equal to those of the corresponding components of TPPP, respectively. (C) Cytotoxicity study on MCF-7 cells incubated with free DTX, PP/DTX (DTX-loaded PP micelles), TPPP, and TPPP/DTX (DTX-loaded TPPP micelles) for 24 h on the basis of various docetaxel concentrations. Experiments were conducted by the MTT method ($n = 3$).

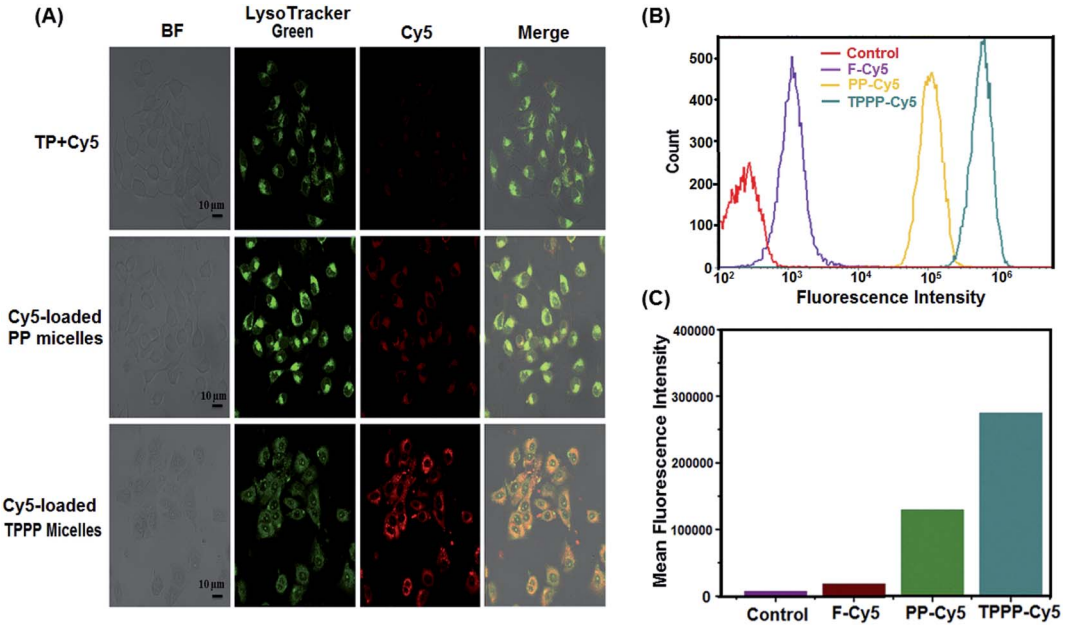

Fig. 7 (A) Confocal images of MCF-7 cells incubated with TP + Cy5, Cy5-loaded PP and Cy5-loaded TPPP micelles for 3 h. Lysosomes were labelled with LysoTracker for 15-20 min before examination. The red and green colors indicate Cy5 and LysoTracker, respectively. (B) Quantitative analysis: cellular uptake of free Cy5 (F-Cy5), Cy5-loaded PP micelles (PP-Cy5) and Cy5-loaded TPPP micelles (TPPP-Cy5) in MCF-7 cells measured by flow cytometry. (C) Mean fluorescence intensity of cellular uptake (2 h). Untreated cells were used as controls. PP = PBAE-PEG, TP = $CGKRK_D(KLAKLAK)_2$, TPPP = $CGKRK_D(KLAKLAK)_2$-PBAE-PEG.

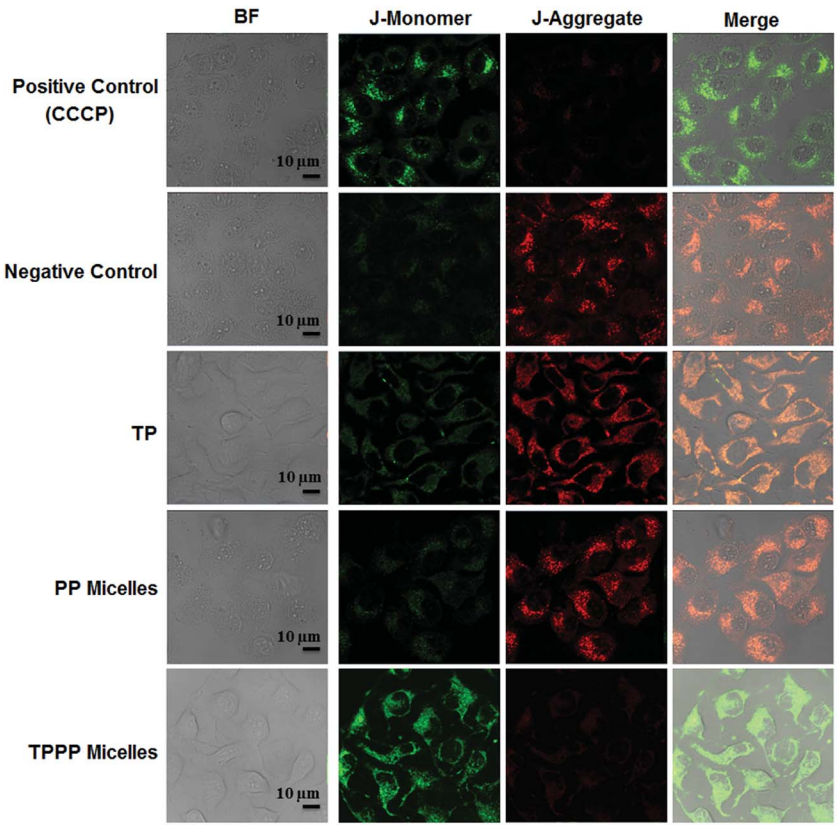

Fig. 8 JC-1 assay in MCF-7 cells treated with TP, PP micelles and TPPP micelles. TP = $CGKRK_D(KLAKLAK)_2$, PP = PBAE-PEG, TPPP = $CGKRK_D(KLAKLAK)_2$-PBAE-PEG.

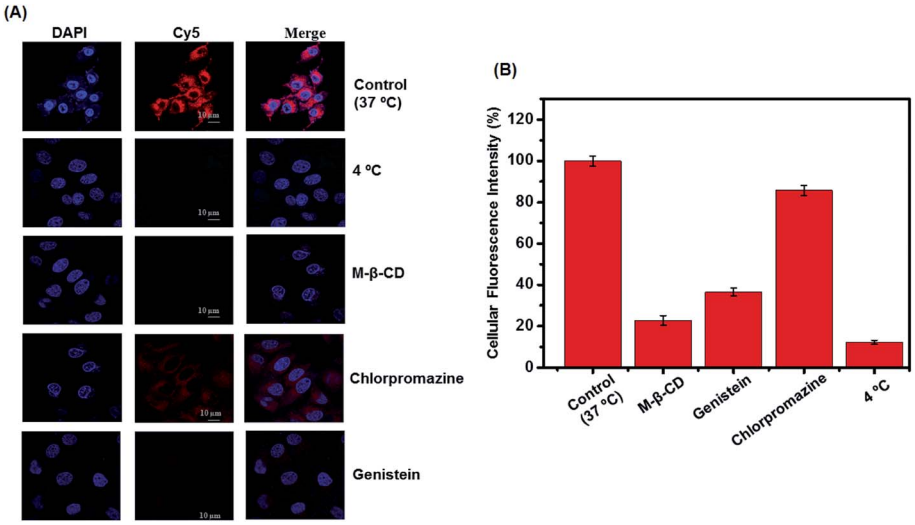

Fig. 9 Evaluation of endocytosis pathways of Cy5-loaded TPPP micelles in MCF-7 cells. (A) Confocal images representing cells treated with various endocytosis inhibitors at 37 °C and controls without any treatment and at 4 °C. The red and blue colors denote Cy5 and DAPI, respectively. (B) Quantitative analysis of fluorescence in MCF-7 cells obtained by Image-Pro Plus 6.0 software ($n = 3$).

1,1′,3,3′-tetraethylbenzimidazolyl carbocyanine iodide (JC-1), which is a fluorescent mitochondrial probe, was used. The probe is cationic and lipophilic in nature, and depending on the mitochondrial transmembrane potential of the cancer cell it accumulates in the cytoplasm as a green monomer or aggregate and emits red fluorescence inside the mitochondria. Fig. 8 illustrates that after incubation with PP micelles and TP for 6 h JC-1 became aggregated in the mitochondria and also at lesser levels in the cytosol. In contrast, after treatment with TPPP micelles the red fluorescence disappeared with an increase in the green fluorescence signal, which indicated serious damage to the mitochondria. Untreated cells were used as negative controls. Carbonyl cyanide *m*-chlorophenylhydrazone (CCCP), which is an uncoupling agent that depolarizes mitochondrial membranes, was selected as a positive control agent.[39]

3.9 Investigation of mechanism of apoptosis

Transmission electron microscopy was used to visualize mitochondrial damage and morphological changes in MCF-7 cells before and after treatment with TPPP micelles. As shown in Fig. S6A,† MCF-7 cells displayed normal morphological features of the mitochondria and nucleus. After incubation with polymeric micelles for 36 h (Fig. S6A†), the mitochondria exhibited abnormal swelling (orange circles), and large vacuoles were found in the cytoplasm (red star).

Furthermore, the nucleus also displayed apoptotic features, *i.e.*, the chromatin was condensed into large dense masses (blue star). In addition to this, we also found electron-dense organelles (yellow star). All these morphological changes represented autophagic characteristics. Finally, loss of the mitochondrial membrane potential led to the apoptotic death of the cancer cells. These data demonstrated that the $CGKRK_D(KLAKLAK)_2$ peptide released from PBAE-PEG was efficiently targeted towards the mitochondria to induce apoptosis *via* the intrinsic mitochondria-dependent apoptosis pathway.

3.10 Micellar internalization pathway

In order to reveal the mechanism of the cellular internalization of TPPP micelles in MCF-7 cells, different endocytosis inhibitors were pre-incubated before treatment with Cy5-loaded TPPP micelles. The inhibitors selected were chlorpromazine (which blocks clathrin-mediated endocytosis), genistein (which blocks caveolae-mediated endocytosis) and M-β-CD (which is a lipid raft inhibitor). A low temperature (4 °C) was also used to determine whether the internalization of the micelles was an active, energy-dependent process. Relevant confocal images are shown in Fig. 9A, and the corresponding quantitative analysis is shown in Fig. 9B. The uptake of TPPP micelles was primarily inhibited by M-β-CD and genistein, which suggested that TPPP micelles were internalized *via* lipid raft-mediated and caveolae-mediated endocytosis pathways. Moreover, cells pre-incubated at 4 °C displayed a tremendous decrease in the uptake of micelles, which suggested that the internalization of micelles was energy-dependent.

4 Conclusions

We have developed dual-targeting copolymeric micelles by conjugating the proapoptotic peptide sequence $CGKRK_D(KLAKLAK)_2$ to the PBAE-PEG polymer. This micellar system recognizes tumor blood vessels and is selectively endocytosed by the cancer cells. Owing to their acidic pH, the micellar system disassembles and is subsequently targeted towards mitochondria to reduce the mitochondrial transmembrane potential and mediate the apoptotic cell death pathway. Here, copolymeric micelles were prepared by dialysis and the hydrophobic anticancer drug DTX was loaded inside the polymeric core. Under mildly acidic conditions, DTX was released from the core to exert its pharmacological role on cancer cells. Therefore, the co-delivery of the mitochondria-targeting $_D(KLAKLAK)_2$ peptide and the microtubulin-targeting drug molecules synergistically

induced the regulated apoptotic cell death of MCF-7 cancer cells. Hence, the pH-sensitive and biodegradable PBAE-PEG copolymeric micelles are considered to be excellent candidates for the co-delivery of the therapeutic peptide and DTX at a targeted tumor site to achieve an enhancement in chemotherapeutic treatment in cancer research.

Acknowledgements

This work was supported by the Natural Science Foundation key project (31630027 and 31430031) and National Distinguished Young Scholars grant (31225009). The authors appreciate the support from the 'Strategic Priority Research Program' of the Chinese Academy of Sciences (XDA09030301), the external cooperation program of BIC, Chinese Academy of Science (121D11KYSB20130006), and the National Natural Science Foundation of China (31600810).

References

1 V. W. van Hinsbergh, A. Collen and P. Koolwijk, *Ann. Oncol.*, 1999, **10**, S60–S63.
2 P. Carmeliet and R. K. Jain, *Nature*, 2000, **407**, 249–257.
3 D. Hanahan and J. Folkman, *Cell*, 1996, **86**, 353–364.
4 N. Ferrara and K. Alitalo, *Nat. Med.*, 1999, **5**, 1359–1364.
5 P. Carmeliet, *Nature*, 2005, **438**, 932–936.
6 E. Ruoslahti, S. N. Bhatia and M. J. Sailor, *J. Cell Biol.*, 2010, **188**, 759–768.
7 E. Ruoslahti, *Nat. Rev. Cancer*, 2002, **2**, 83–90.
8 T. M. Allen and P. R. Cullis, *Science*, 2004, **303**, 1818–1822.
9 R. K. Jain, L. E. Gerlowski and E. V. Cilento, *Crit. Rev. Oncol. Hematol.*, 1986, **5**, 115–170.
10 T. Wei, J. Liu, H. Ma, Q. Cheng, Y. Huang, J. Zhao, S. Huo, X. Xue, Z. Liang and X.-J. Liang, *Nano Lett.*, 2013, **13**, 2528–2534.
11 H. Kulhari, D. Pooja, S. Shrivastava, S. R. Telukutala, A. K. Barui, C. R. Patra, G. M. N. Vegi, D. J. Adams and R. Sistla, *Nanomedicine*, 2015, **11**, 1511–1520.
12 M. Potente, H. Gerhardt and P. Carmeliet, *Cell*, 2011, **146**, 873–887.
13 J. A. Hoffman, E. Giraudo, M. Singh, L. Zhang, M. Inoue, K. Porkka, D. Hanahan and E. Ruoslahti, *Cancer Cell*, 2003, **4**, 383–391.
14 T. A. Järvinen and E. Ruoslahti, *Am. J. Pathol.*, 2007, **171**, 702–711.
15 V. Fogal, L. Zhang, S. Krajewski and E. Ruoslahti, *Cancer Res.*, 2008, **68**, 7210–7218.
16 L. Agemy, D. Friedmann-Morvinski, V. R. Kotamraju, L. Roth, K. N. Sugahara, O. M. Girard, R. F. Mattrey, I. M. Verma and E. Ruoslahti, *Proc. Natl. Acad. Sci. U. S. A.*, 2011, **108**, 17450–17455.
17 L. Agemy, V. R. Kotamraju, D. Friedmann-Morvinski, S. Sharma, K. N. Sugahara and E. Ruoslahti, *Mol. Ther.*, 2013, **21**, 2195–2204.
18 M. M. Javadpour, M. M. Juban, W.-C. J. Lo, S. M. Bishop, J. B. Alberty, S. M. Cowell, C. L. Becker and M. L. McLaughlin, *J. Med. Chem.*, 1996, **39**, 3107–3113.
19 S. Foillard, Z. h. Jin, E. Garanger, D. Boturyn, M. C. Favrot, J. L. Coll and P. Dumy, *ChemBioChem*, 2008, **9**, 2326–2332.
20 K. Karjalainen, D. E. Jaalouk, C. E. Bueso-Ramos, A. J. Zurita, A. Kuniyasu, B. L. Eckhardt, F. C. Marini, B. Lichtiger, S. O'Brien and H. M. Kantarjian, *Blood*, 2011, **117**, 920–927.
21 J. C. Mai, Z. Mi, S.-H. Kim, B. Ng and P. D. Robbins, *Cancer Res.*, 2001, **61**, 7709–7712.
22 K. Rege, S. J. Patel, Z. Megeed and M. L. Yarmush, *Cancer Res.*, 2007, **67**, 6368–6375.
23 S. Kim, G. S. Kim, J. Seo, G. Gowri Rangaswamy, I.-S. So, R.-W. Park, B.-H. Lee and I.-S. Kim, *Biomacromolecules*, 2015, **17**, 12–19.
24 W. Arap, W. Haedicke, M. Bernasconi, R. Kain, D. Rajotte, S. Krajewski, H. M. Ellerby, D. E. Bredesen, R. Pasqualini and E. Ruoslahti, *Proc. Natl. Acad. Sci. U. S. A.*, 2002, **99**, 1527–1531.
25 H. M. Ellerby, W. Arap, L. M. Ellerby, R. Kain, R. Andrusiak, G. Del Rio, S. Krajewski, C. R. Lombardo, R. Rao and E. Ruoslahti, *Nat. Med.*, 1999, **5**, 1032–1038.
26 X. Ma, X. Wang, M. Zhou and H. Fei, *Adv. Healthcare Mater.*, 2013, **2**, 1638–1643.
27 Y. Shamay, L. Adar, G. Ashkenasy and A. David, *Biomaterials*, 2011, **32**, 1377–1386.
28 K. Engin, D. Leeper, J. Cater, A. Thistlethwaite, L. Tupchong and J. McFarlane, *Int. J. Hyperthermia*, 1995, **11**, 211–216.
29 E. S. Lee, K. T. Oh, D. Kim, Y. S. Youn and Y. H. Bae, *J. Controlled Release*, 2007, **123**, 19–26.
30 M. Stubbs, P. M. McSheehy, J. R. Griffiths and C. L. Bashford, *Mol. Med. Today*, 2000, **6**, 15–19.
31 D. M. Lynn and R. Langer, *J. Am. Chem. Soc.*, 2000, **122**, 10761–10768.
32 S. Tang, Q. Yin, Z. Zhang, W. Gu, L. Chen, H. Yu, Y. Huang, X. Chen, M. Xu and Y. Li, *Biomaterials*, 2014, **35**, 6047–6059.
33 K. H. Min, J.-H. Kim, S. M. Bae, H. Shin, M. S. Kim, S. Park, H. Lee, R.-W. Park, I.-S. Kim and K. Kim, *J. Controlled Release*, 2010, **144**, 259–266.
34 M. S. Kim, S. J. Hwang, J. K. Han, E. K. Choi, H. J. Park, J. S. Kim and D. S. Lee, *Macromol. Rapid Commun.*, 2006, **27**, 447–451.
35 I. H. Van Stokkum, H. J. Spoelder, M. Bloemendal, R. Van Grondelle and F. C. Groen, *Anal. Biochem.*, 1990, **191**, 110–118.
36 M. S. Kim, G. H. Gao, S. W. Kang and D. S. Lee, *Macromol. Biosci.*, 2011, **11**, 946–951.
37 K. Akiyoshi, S. Deguchi, H. Tajima, T. Nishikawa and J. Sunamoto, *Macromolecules*, 1997, **30**, 857–861.
38 C. L. Zhao, M. A. Winnik, G. Riess and M. D. Croucher, *Langmuir*, 1990, **6**, 514–516.
39 P. Heytler, *Biochemistry*, 1963, **2**, 357–361.

